Control of a Seven-phase Axial Flux Machine Designed for Fault Operation

F. Locment, E. Semail, X. Kestelyn, A. Bouscayrol
L2EP ENSAM
8 Bd Louis XIV
Lille 59046
FRANCE
eric.semail@lille.ensam.fr

***Abstract* – This paper deals with control in fault operation of a seven-phase Permanent Magnet Synchronous Machine supplied by a seven-leg Voltage Source Inverter (VSI). Using a Multi-Machine description, a seven-phase machine which presents a special ability to be controlled with only five phases supplied has been designed. The machine is presented and experimental results are provided when two phases are opened. In a first case of no change of classical control, high torque ripples are observed. In a second case, a specific control deduced from the Multi-Machine modelling is suggested for reducing torque ripples.**

I. INTRODUCTION

Multiphase machines suffer from an apparent higher number of switching devices than three-phase ones. Nevertheless, in high power applications such as electrical ships [1] or low voltage/high current applications such as on-board traction systems [2]-[3], this drawback is not so obvious: the use of high current devices implies high heat dissipation capabilities especially with high frequencies. In these cases parallel converters or parallel/series device associations are often used.

Moreover, when reliability is required such as in aircraft [4], in marine applications [5], multiphase drives [6] must be considered as an alternative to three-phase multi-level converter drives whose reconfiguration in safety mode is not obvious.

Contrary to three-phase wye-connected machines, the loss of one phase is not critical for seven-phase machines. However, torque ripples appear with usual vector control of the machine [5]-[7]. The magnitude of the ripples depends on the interaction between the non-symmetrical system of currents and the symmetrical system of electromotive forces (EMF). In [8], new references of the currents are determined and corresponding currents are obtained using to hysteresis controllers in stator frame. However in this case the carrier frequency of the Pulse Width Modulation (PWM) VSI is not constant which is damaging for electromagnetic compatibility. In [7], two models are used. The first one is dedicated to normal operation. A second model is defined for fault operation using a new transformation. In this case, the control of currents is then achieved in a new synchronous frame with Proportional Integral (PI) controllers which have constant references in steady states. The errors are then equal to zero. However, the change of synchronous frame depends on the kind of fault.

In this paper, the same model is used for normal and fault operations. Thus the same control structure is used in both operation modes using PI controllers in the synchronous frame. Such a fault operation control is possible because the machine has been specifically designed.

This control strategy is deduced from a Multi-Machine Multi-Converter modelling of the seven-phase machine supplied by seven-leg VSI [9]. In this modelling method, the seven-phase machine can be considered as a set of three (dq) fictitious machines. Mathematically, this approach is close to multi-reference frame one [10] but highlights physical couplings which have to be taken into account by the control. The mathematical basis of the two approaches, introduced for six-phase machines [11], is the same: the existence of subspaces associated with the eigenvalues of stator inductance matrix.

From the suggested model, constraints on the control but also on the machine are deduced. A seven-phase NN TORUS machine has been made using analytical and 3D-Finite Element Methods [12]-[13]. Experimental results of the implemented control are provided when two phases are not supplied. Using the same PI controllers as in normal operation it is shown that torque ripples can be weak if reference currents are adapted. At last, reduction of torque ripples is obtained using a specific control deduced from the Multi-Machine model.

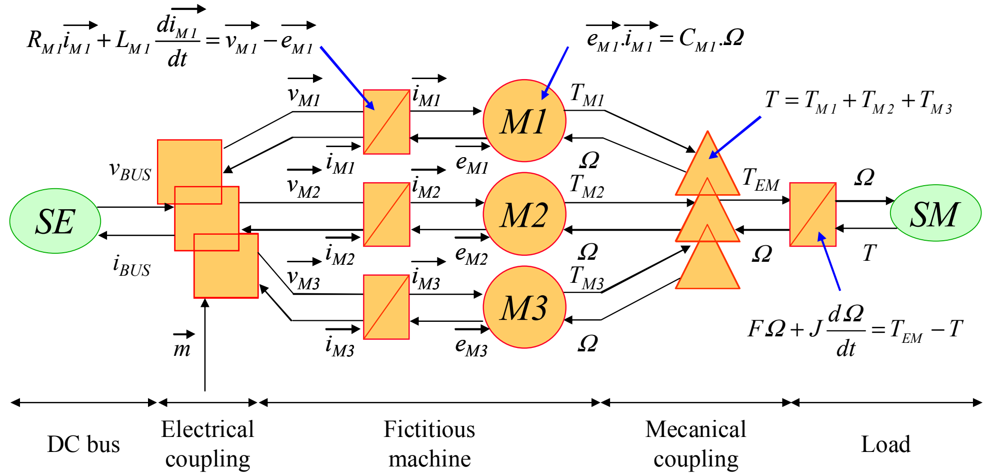

Fig. 1. Multi-Machine Energetic Macroscopic Representation of the seven-phase machine

II. MULTI-MACHINE VECTORIAL CHARACTERIZATION

Under assumptions of no saturation, no reluctance effects and regularity of design, a vectorial formalism allows to prove that a seven-phase machine is equivalent to a set of three magnetically independent fictitious two-phase machines [9] named *M1*, *M2* and *M3*. Each equivalent machine is characterized by its resistance (resp. R_{M1}, R_{M2} and R_{M3}), inductance (resp. L_{M1}, L_{M2} and L_{M3}), and EMF (resp. $\overrightarrow{e_{M1}}$, $\overrightarrow{e_{M2}}$ and $\overrightarrow{e_{M3}}$).

The torque of the real machine T, is the sum of the torque of these three fictitious machines T_{M1}, T_{M2} and T_{M3}. The seven-leg VSI can also be decomposed into three fictitious VSI electrically coupled by a mathematical transformation Concordia-type:

$$[C_7]=\sqrt{\frac{2}{7}}\begin{bmatrix} \frac{1}{\sqrt{2}} & 1 & 0 & 1 & 0 & 1 & 0 \\ \frac{1}{\sqrt{2}} & \cos\frac{2\pi}{7} & \sin\frac{2\pi}{7} & \cos\frac{4\pi}{7} & \sin\frac{4\pi}{7} & \cos\frac{6\pi}{7} & \sin\frac{6\pi}{7} \\ \frac{1}{\sqrt{2}} & \cos\frac{4\pi}{7} & \sin\frac{4\pi}{7} & \cos\frac{8\pi}{7} & \sin\frac{8\pi}{7} & \cos\frac{12\pi}{7} & \sin\frac{12\pi}{7} \\ \frac{1}{\sqrt{2}} & \cos\frac{6\pi}{7} & \sin\frac{6\pi}{7} & \cos\frac{12\pi}{7} & \sin\frac{12\pi}{7} & \cos\frac{18\pi}{7} & \sin\frac{18\pi}{7} \\ \frac{1}{\sqrt{2}} & \cos\frac{8\pi}{7} & \sin\frac{8\pi}{7} & \cos\frac{16\pi}{7} & \sin\frac{16\pi}{7} & \cos\frac{24\pi}{7} & \sin\frac{24\pi}{7} \\ \frac{1}{\sqrt{2}} & \cos\frac{10\pi}{7} & \sin\frac{10\pi}{7} & \cos\frac{20\pi}{7} & \sin\frac{20\pi}{7} & \cos\frac{30\pi}{7} & \sin\frac{30\pi}{7} \\ \frac{1}{\sqrt{2}} & \cos\frac{12\pi}{7} & \sin\frac{12\pi}{7} & \cos\frac{24\pi}{7} & \sin\frac{24\pi}{7} & \cos\frac{36\pi}{7} & \sin\frac{36\pi}{7} \end{bmatrix},\quad(1)$$

A key of the problem is that each one of the 2-phase fictitious machine, associated with a vectorial subspace S_k, is characterized by an harmonic family (Table I). The three subspaces are orthogonal each other. It is this orthogonality which allows to introduce the concept of fictitious machine. For a seven-phase machine, as there are three fictitious machines, as least three spatial harmonics, one per machine, should be considered in order to correctly design the machine.

To get a synthetic graphical representation, a formalism (Energetic Macroscopic Representation, EMR) developed from Multi-Machine Multi-Converter study [14], is used (see Appendix and Fig. 1). Interleaved triangles (resp. squares) highlight a mechanical (resp. electrical) coupling between the three fictitious machines.

TABLE I
HARMONIC CHARACTERIZATION OF FICTITIOUS MACHINES FOR WYE-CONNECTED SEVEN-PHASE MACHINE

Fictitious 2-phase machines	Families of odd harmonics
M1	$\mathbf{1}, 13, 15, \ldots, 7h\pm 1$
M2	$\mathbf{5}, 9, 19, \ldots, 7h\pm 2$
M3	$\mathbf{3}, 11, 17, \ldots, 7h\pm 3$

III. PRESENTATION, DESIGN AND CHARACTERIZATION OF MACHINE FOR CONTROL

A. Presentation of the axial flux seven-phase machine

A six-pole seven-phase NN TORUS [15] machine with two external rotors has been designed. Fig. 2 shows one sixth of the studied axial flux seven-phase machine. The stator, with Gramme-ring windings, is soft magnetic composite made with 42 slots (Fig. 3). Its external diameter is of 287 mm and thickness of 123 mm. It is designed for a nominal torque of 65 Nm.

B. Design of the seven-phase axial flux machine

When two phases are not supplied, two currents can not be controlled any more. There remains only four degrees of freedom for the control. Consequently, it is possible to impose currents in only two of the three two-phase fictitious machines. The two currents of one of these two-phase machines can not be controlled. If the EMF of this non-controlled machine are not equal to zero, torque ripples are then induced. Therefore, we have imposed, during the design, to minimize the harmonics of this machine. We have chosen *M2* among the three machines because *M1* and *M3* have more potential for torque production since the main harmonics associated with them are the first and the third ones (TABLE I).

To eliminate the fifth harmonic from the fictitious machine *M2* (see TABLE I), we set up a 4/5 pole arc within the magnet repartition (Fig. 3).

C. Characterization of the seven-phase axial flux machine

Fig. 4 shows EMF of phase A, the harmonic spectrum is presented in Table II (for a speed of 275 rpm). For harmonics higher than 9, the relative RMS values are less than 3 %. The fifth harmonic is almost equal to zero. However the ninth harmonic which represents still 6.2% of the first harmonic will induce torque ripple in the machine.

TABLE II
MEASURED HARMONIC BREAKDOWN OF EMF

Order of harmonic	1	3	5	7	9
Relative RMS values	100%(40V)	21%	0.4%	6.9%	6.2%

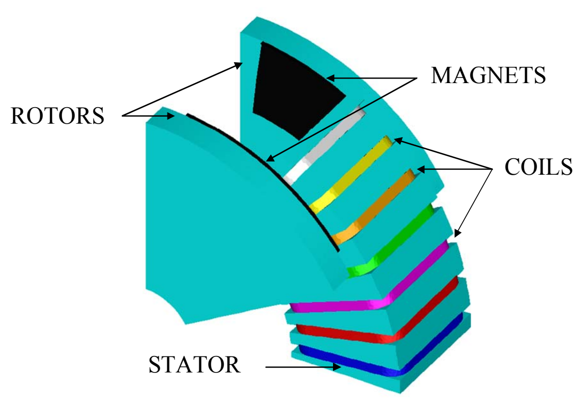

Fig. 2. One sixth of the axial flux seven-phase machine

Fig. 3. Stator and rotor of the studied machine

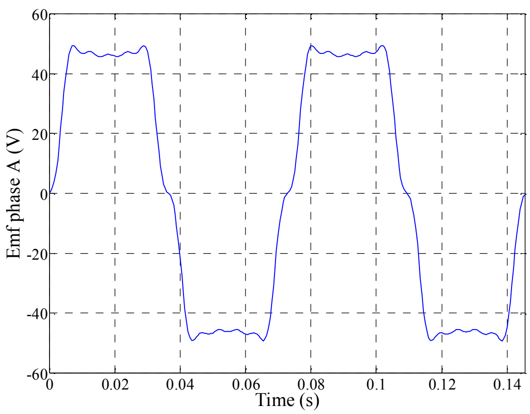

Fig. 4. Measured EMF of phase A at 275 rpm

IV. CONTROL OF MACHINE IN FAULT OPERATION

In Fig. 5, we present the structure of control deduced from the presented model (see Appendix) using causality properties. Three control blocks allow to impose independently the currents in the three fictitious machines. PI current controllers are used for each fictitious machine since control is achieved in synchronous frame.

The considered fault operation supposes that currents in phase A and B are cancelled. The objective is to keep the same controllers for the currents and to change only their references in order to minimize the torque ripples.

Fig. 1 shows that the electromechanical conversion can be expressed by equation (2):

$$\overrightarrow{e_{M1}}.\overrightarrow{i_{M1}} = T_{M1}\Omega \qquad \overrightarrow{e_{M2}}.\overrightarrow{i_{M2}} = T_{M2}\Omega \qquad \overrightarrow{e_{M3}}.\overrightarrow{i_{M3}} = T_{M3}\Omega\,, \tag{2}$$

with:

$$\begin{cases}\overrightarrow{e_{M1}} = \left[e_{M1\alpha}\, e_{M1\beta}\right]^t \\ \overrightarrow{i_{M1}} = \left[i_{M1\alpha}\, i_{M1\beta}\right]^t\end{cases} \quad \begin{cases}\overrightarrow{e_{M2}} = \left[e_{M2\alpha}\, e_{M2\beta}\right]^t \\ \overrightarrow{i_{M2}} = \left[i_{M2\alpha}\, i_{M2\beta}\right]^t\end{cases} \quad \begin{cases}\overrightarrow{e_{M3}} = \left[e_{M3\alpha}\, e_{M3\beta}\right]^t \\ \overrightarrow{i_{M3}} = \left[i_{M3\alpha}\, i_{M3\beta}\right]^t\end{cases}, \tag{3}$$

We suppose that the design of the machine allows to consider that $\overrightarrow{e_{M2}} = \vec{0}$. In this case, there is no torque induced by $\overrightarrow{i_{M2}}$. The torque can be produced only by *M1* and *M3* machines. The harmonic characterization of the machine shows that the *M1* and *M3* machines have sinusoidal EMF: the vectors $\overrightarrow{e_{M1}}$ (resp. $\overrightarrow{e_{M3}}$) have a constant magnitude and rotate at speed ω (resp. 3ω) with $\omega = 3\Omega$. To get constant torque in these machines it is then sufficient to impose vectors $\overrightarrow{i_{M1}}$ and $\overrightarrow{i_{M3}}$ with constant modulus and a rotation at the same speed as the vectors $\overrightarrow{e_{M1}}$ and $\overrightarrow{e_{M3}}$. The reference of currents in the fictitious machines *M1* and *M3* are chosen equal to:

$$\begin{cases} i_{M1\alpha} = I_{M1}\sin(\omega t) \\ i_{M1\beta} = -I_{M1}\cos(\omega t) \\ i_{M3\alpha} = 0 \\ i_{M3\beta} = 0 \end{cases} \tag{4}$$

In order to keep the same controller as in normal operation, it is necessary to find the vector $\overrightarrow{i_{M2}}$ that will exist in fault operation. It will be then sufficient to impose the corresponding references to the current controller associated with the *M2* machine.

Taking into account (4), we have to solve (5):

$$[C_7].\begin{bmatrix} 0 \\ I_{M1}\sin(\omega t) \\ -I_{M1}\cos(\omega t) \\ i_{M2\alpha} \\ i_{M2\beta} \\ 0 \\ 0 \end{bmatrix} = \begin{bmatrix} i_A \\ i_B \\ i_C \\ i_D \\ i_E \\ i_F \\ i_G \end{bmatrix} = \begin{bmatrix} 0 \\ 0 \\ i_C \\ i_D \\ i_E \\ i_F \\ -(i_C + i_D + i_E + i_F) \end{bmatrix}, \tag{5}$$

The results are:

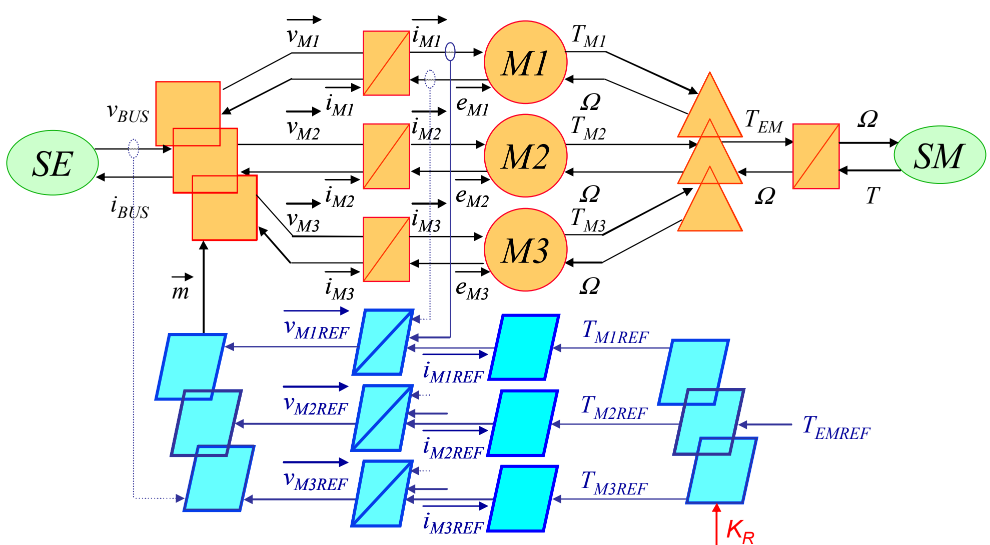

Fig. 5. Structure of control

$$\begin{cases} i_{M2\alpha} = -I_{M1}\sin(\omega t) \\ i_{M2\beta} = I_{M1}\left(0.8\cos(\omega t) - 0.87\sin(\omega t)\right) \end{cases}, \tag{6}$$

For example, for the studied fault operation and improved control, we have in Fig. 6 the currents in the three fictitious machines and in Fig. 7 the currents in the real machine. It can be noted that i_E is much more higher than in normal operation: in fault operation a reduced torque must be required.

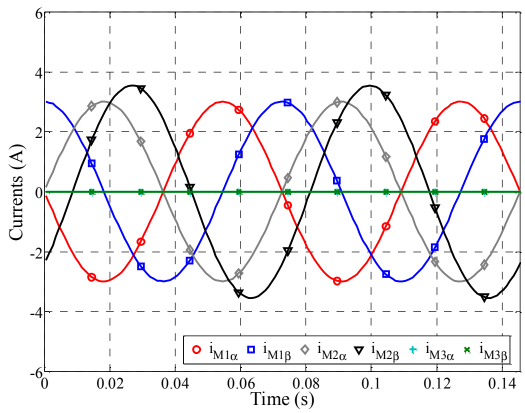

Fig. 6. Currents of the three fictitious machines in fault operation and improved control ($I_{M1} = 3A$)

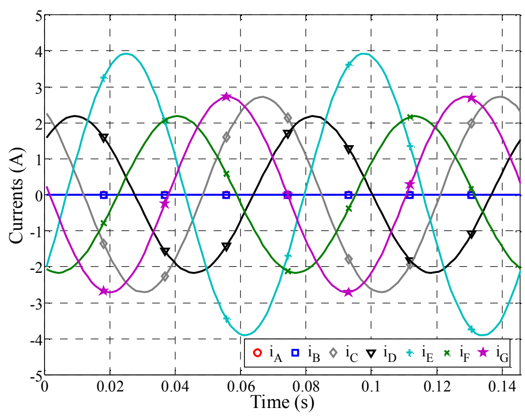

Fig. 7. Currents of the real machine in fault operation and improved control

V. EXPERIMENTAL RESULTS

All the results are obtained with PI controllers for torque control of each fictitious machine. The PWM frequency of the inverter is set to 20 kHz with a usual triangle intersection method is used. There is only a torque control, no speed control.

In normal operation at 275 rpm, the average torque is equal to 19.5 Nm. The corresponding currents are given in Fig. 8. A vector control is chosen in order to minimize copper losses for a given torque.

At constant speed, the loss of two phases produces an unbalanced system of currents (Fig. 11). The corresponding torque measured with a torque sensor (TORQUEMASTER TM211) is shown in Fig. 9 (subscript DM1 in blue). The torque ripple magnitude reaches 24 Nm (Fig. 10) with a high second harmonic amplitude. However the machine is still rotating.

To decrease this torque ripple, we apply the new current set point in the *M2* fictitious machine as given in (6). Fig. 12 shows that the five remaining currents in the multi-phase machine tend to balance but with higher amplitude than in normal operation. Measured currents are very close to predicted currents (see Fig. 7). With this modification of control, the torque ripple decreases drastically and is equal to 3.5 Nm (Fig. 9 and Fig. 10).

The torques in normal and fault operations are not completely identical because the currents of the *M3* fictitious machine (Fig. 15) and EMF of the *M2* fictitious machine (TABLE II) are not null. Therefore, *M2* and *M3* produce torque ripples.

Then we compare constraints on currents for the different studied cases (Fig. 11 and Fig. 12). We can see that the maximum amplitude of current is observed in the case of improved control of torque: about 4 A peak for i_E instead of 3 A peak in unchanged control for i_C.

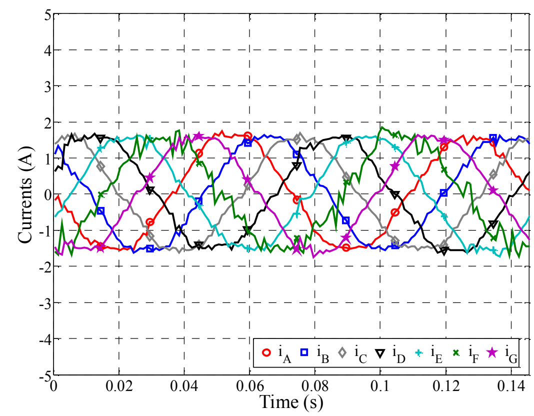

Fig. 8. Measured currents in normal operation

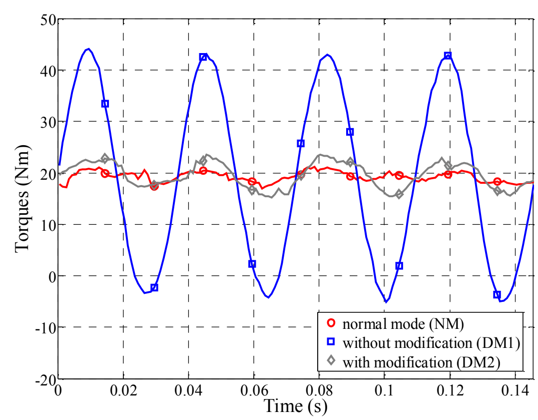

Fig. 9. Experimental torques in the seven-phase machine

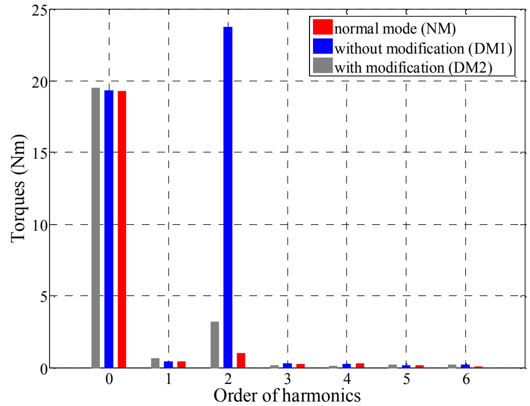

Fig. 10. Spectral analysis of torques

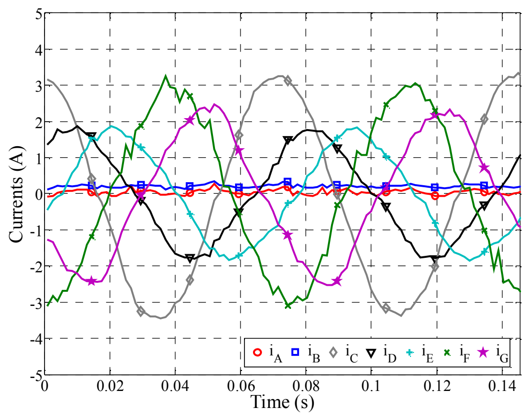

Fig. 11. Measured currents in fault operation without change of control

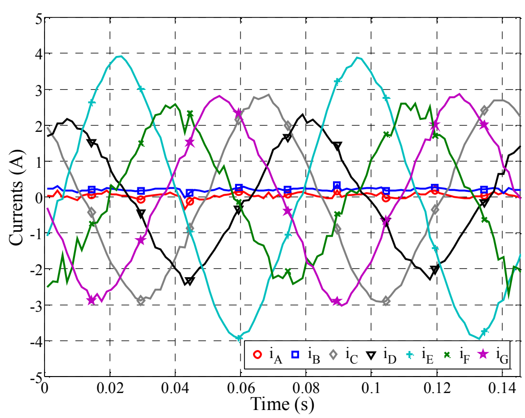

Fig. 12. Measured currents in fault operation with improved control

For improved fault operation (subscript DM2), the torque references are the same as in normal operation for *M1* and *M3*. It can be verified that currents in *M1* and *M3* are unchanged (Fig. 13 and Fig. 14) and close to those predicted (see Fig. 6).

For the *M2* machine, reference currents (Fig. 6) and measured currents (Fig. 15) are also very close. In normal mode, the currents are almost equal to zero. In fault operation with improved control, currents are injected in order to suppress torque ripples.

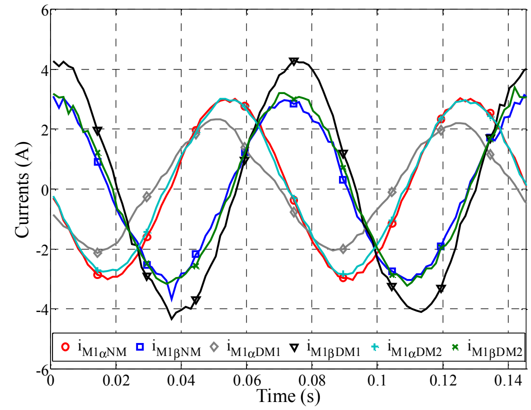

Fig. 13. Currents of *M1* for the three studied cases

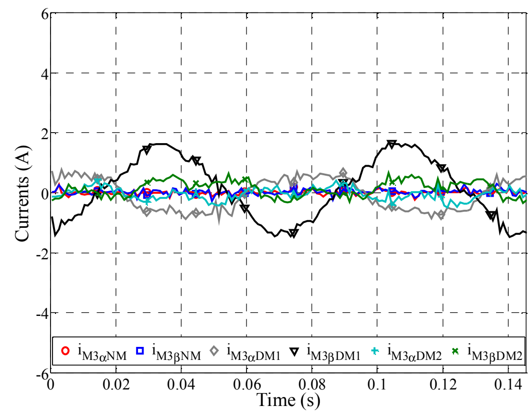

Fig. 14. Currents in *M3* for the three studied cases

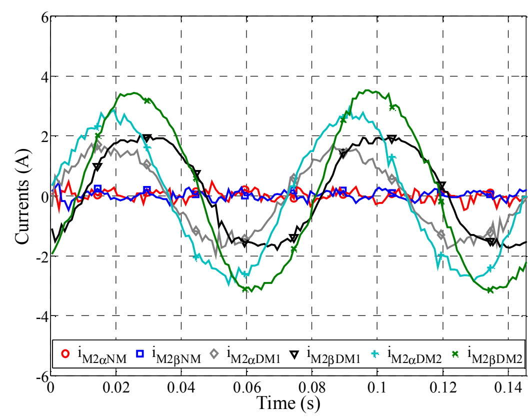

Fig. 15. Currents of *M2* for the three studied cases

VI. CONCLUSION

In this paper the tolerance to a fault operation has been validated for a seven-phase machine. These results have been obtained by using a specific design of the machine. One interest with this machine is that neither the structure of the control nor the PI-controllers have to be changed between the normal and fault operations. A modification of the current references in a fictitious machine *M2* has only to be calculated to reduce drastically the torque ripples which appear when two phases are opened. In this machine *M3* the references are not constant but it is no a matter since the EMF is equal to zero. For the two others machines the references remain constant. In this paper, a particular case has been chosen (phase A and B opened) but the approach can be extended when one phase or two other phases are opened. However, as the EMF of the *M3* machine is not equal to zero the extension to more than two phases opened is not so easy.

VII. REFERENCES

[1] S. Siala, E. Guette and J. L. Pouliquen, "Multi-inverter PWM control: a new generation drives for cruise ship electric propulsion", *Proc. of EPE'03*, Toulouse (France), Sept. 2003, CD-ROM.

[2] G. Simões and P. Vieira, "A High-Torque Low-Speed Multiphase Brushless Machine — A Perspective Application for electric vehicles ", *IEEE Trans. on Industrial Electronics*, vol. 49, no. 5, Oct. 2002, pp. 1154-1164.

[3] M. Abolhassani, "A novel Multiphase Fault Tolerant High Torque Density Permanent Magnet Motor Drive for Traction Application", *Proc. of IEEE-IEMDC'05*, San Antonio (USA), May 2005, pp. 728 - 734.

[4] J.W. Bennett, A.G. Jack, B.C. Mecrow, D.J. Atkinson, C. Sewell and G. Mason, "Fault-tolerant Control Architecture for an Electrical Actuator", *Proc. of IEEE-PESC'04*, Aachen (Germany), June 2004, pp. 4371-4377, Vol.6.

[5] J. Wang, K. Atallah and D. Howe, "Optimal torque control of fault-tolerant permanent magnet brushless machines", *IEEE Trans. on Magnetics*, vol. 39, no. 5, Sept 2003, pp. 2962-2964.

[6] T.M. Jahns, "Improved reliability in solid state ac drives by means of multiple independent phase-drive units", *IEEE Trans. on Industry Applications*, vol. IA-16, May-June 1980, pp. 321-331.

[7] H-M Ryu, J-H Kim and S-K Sul, "Synchronous Frame Current Control of Multi-Phase Synchronous Motor, Part II. Asymmetric Fault Condition due to Open Phases", *Proc. of IEEE-IAS'04*, Vol. 1, pp. 268-275, Seattle (USA), Oct. 2004.

[8] L. Parsa and H. A. Toliyat, "Fault-Tolerant Five-Phase Permanent Magnet Motor Drives", *Proc. of IEEE-IAS'04*, Vol.2, pp. 1048-1054, Seattle (USA), Oct. 2004.

[9] E. Semail, X. Kestelyn, and A. Bouscayrol, "Right Harmonic Spectrum for the back-electromotive force of a n-phase synchronous motor", *Proc. of IEEE-IAS'04*, Vol. 1, pp.71-78, Seattle (USA), Oct. 2004.

[10] H-M Ryu, J-W Kim and S-K Sul, "Synchronous Frame Current Control of Multi-Phase Synchronous Motor, Part I. Modeling and Current Control Based on Multiple d-q Spaces Concept Under Balanced Condition", *Proc. of IEEE-IAS'04,* Vol. 1, pp. 56-63, Seattle (USA), Oct. 2004.

[11] Y. Zhao and T. Lipo, "Space Vector PWM Control of Dual Three-Phase Induction Machine Using Space Vector Decomposition", *IEEE Trans. on Industry Applications,* vol. 31, no. 5, Sept./Oct. 1995, pp. 1100-1109.

[12] F. Locment, E. Semail and F. Piriou, "Design and Study of a Multi-phase Axial-flux machine", *IEEE Trans. on Magnetics*, vol. 42, no. 4, pp. 1427-1430, April 2006.

[13] F. Locment, E. Semail and F. Piriou, "Soft Magnetic Composite Axial Flux Seven-Phase Machine", *Proc. of ICEM'06,* Chania, (Greece), Sept. 2006, CD-ROM.

[14] A. Bouscayrol, B. Davat, B. de Fornel, B. François, J. P. Hautier, F. Meibody-Tabar and M. Pietrzak-David, "Multimachine Multiconverter System: application for electromechanical drives", *European Physics Journal - Applied Physics*, vol. 10, no. 2, May 2000, pp. 131-147.

[15] S. Huang, M. Aydin and T.A. Lipo, "TORUS Concept Machines: Pre-Prototyping Assessment for Two Major Topologies", *Proc. of IEEE-IAS'01*, Chicago (USA), Oct. 2001, pp. 1619-1625.

Appendix: Synoptic of Energetic Macroscopic Representation

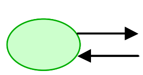 Source of energy	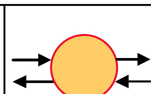 Electromechanical converter (without energy accumulation)	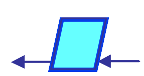 Control block without controller
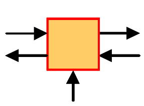 Electrical converter (without energy accumulation)	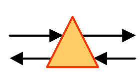 Mechanical converter (without energy accumulation)	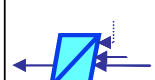 Control block with controller
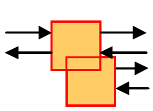 Electrical coupling (without energy accumulation)	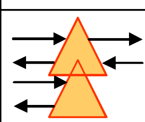 Mechanical coupling (without energy accumulation)	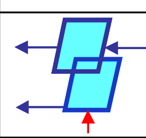 Control block with coupling criterion
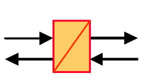 Element with energy accumulation		